SILICA PHASE AS A THERMOLUMINESCENCE PHOSPHOR IN ALH-77214 (L3.4) CHONDRITE

Satoshi MATSUNAMI[1], Kiyotaka NINAGAWA[2], Hideyuki KUBO[2], Shin-ichi FUJIMURA[2], Isao YAMAMOTO[2], Tomonori WADA[3] and Hiroshi NISHIMURA[1]

[1] *Naruto University of Education, Takashima, Naruto 772*
[2] *Okayama University of Science, 1–1, Ridai-cho, Okayama 700*
[3] *Okayama University, 1–1, Tsushimanaka 3-chome, Okayama 700*

Abstract: The induced thermoluminescence (TL) images for a slice sample of ALH-77214 (L3.4) have been measured to examine TL phosphors in type 3 ordinary chondrites with low TL sensitivity, using a TL spatial distribution readout system combined with microscope. The chemical compositions of TL phosphors were analyzed by X-ray microanalyzer.

The TL emissions due to silica phases have been newly observed in two pyroxene chondrules with silica inclusions ($SiO_2=97$–99 wt%) and one porphyritic olivine chondrule with very silica-rich mesostasis ($SiO_2=84$ wt%), in addition to those due to feldspar crystals formed in chondrule mesostases enriched in plagioclase component. The glow curves of the silica phases (the peaks around 240–280°C) are quite different from those of the usual chondrule mesostases (the peaks around 80–120°C). We have tried to utilize glow curves of induced TL for five silica phases (hydrothermal quartz, volcanic quartz, tridymite, cristobalite and silica glass). From similarities of the shape of glow curve, the silica phase was tentatively identified to be cristobalite. Utilizing silica phases as a common TL phosphor, we can make a comparative study of TL characteristics among chondritic meteorites.

1. Introduction

SEARS *et al.* (1980) have made a great progress in quantitative classification of type 3 ordinary chondrites, which have been classified into petrologic subtypes, ranging from 3.0 to 3.9, using the thermoluminescence (TL) sensitivity (SEARS *et al.*, 1980, 1982, 1991; SEARS and WEEKS, 1983). The minerals responsible for the TL have been interpreted to be mainly feldspars that recrystallized in chondrule mesostases owing to metamorphism (SEARS *et al.*, 1982, 1984; SEARS, 1988).

NINAGAWA *et al.* (1990) have successfully obtained the natural TL images of ordinary chondrites with high TL sensitivity (ALH-77294 (H5) and ALH-77216 (L3.8)) by a TL spatial distribution readout system combined with microscope. Recently, NINAGAWA *et al.* (1991) have reported induced TL images of one equilibrated ordinary chondrite (EOC) (ALH-78043 (L6)) and three type-3 ordinary chondrites (ALH-77214 (L3.4), Yamato-74191 (L3.6) and ALH-77216 (L3.8)). Moreover, chemical compositions of the TL phosphors have been obtained by X-ray microanalyzer (EPMA). Their works clearly indicate that chondrule mesostases enriched in plagioclase component are mainly responsible for the TL

270

emission in these chondrites and that the peak temperature and peak width of glow curve are positively correlated with molar ratio ab/(ab + an) in terms of normative minerals.

In this paper, we report a finding of the TL emissions due to silica phases in ALH-77214 chondrite with low TL sensitivity. It is revealed that the silica phases have strikingly different TL characteristics from those of chondrule mesostases enriched in plagioclase component. The silica polymorph has been also determined tentatively. We briefly discuss the importance of silica phases as a common TL phosphor in chondritic meteorites.

2. Experimental

Thick slice samples of ALH-77214 (L3.4) chondrite were prepared. They were fixed onto metallic plates by epoxy resin and polished carefully with alumina abrasives to about 1 mm thickness and finally with diamond paste (diameter of diamond grain ~1 μm). The samples were irradiated by ^{60}Co γ-rays and received a dose of 13.2 kGy, because ALH-77214 (L3.4) chondrite is considered to have low TL sensitivity (SEARS et al., 1982, 1991). The TL measurements were conducted immediately after γ-rays irradiation, at the heating rate 0.25°C/s with a Corning band pass filter 4–96 in nitrogen atmosphere. The TL spatial distribution readout system combined with microscope has been already described by NINAGAWA et al. (1990). The TL images at various temperatures were readout to obtain temperature variation of the TL spatial distribution.

After the TL measurements, polished surfaces of the slice samples were observed in detail by scanning electron microscope (SEM) in both secondary electron and backscattered electron modes. Backscattered electron images (BEI) of the samples were fully utilized. By careful comparison of the TL images with BEI, we determined the positions with high TL emission at various temperatures. Analyses of chemical compositions of these positions were performed on the automated JCXA-733 (JEOL) instrument by routine wavelength dispersive procedures. Operating conditions were 15 kV accelerating voltage, 12 nA beam current, a focussed beam diameter of about 1 μm for point analyses of olivine and pyroxenes. Analyses of mesostases and silica-rich phases were conducted using defocussed beams of 5–10 μm in diameter. The conventional ZAF correction procedures were employed. In the case of analyses for mesostases and silica, relatively low sums (95–98%) were obtained in many analyses, but these appear to be systematic and do not reflect missing elements. This is presumably because of incomplete polishing of chondrule mesostases. Therefore, average compositions were calculated and listed for analytical data recalculated to total 100%.

3. Results

3.1. Temperature variation of TL spatial distribution

A slice sample of ALH-77214 is shown in Fig. 1a. The TL images at 100 and 250°C are selected to show temperature variation of TL spatial distribution

(Figs. 1b and c). Six square portions (I, II, III, IV, V, and VI) are also illustrated in these figures. As clearly shown in Fig. 1, the positions with intense TL emission are not uniformly distributed and are restricted to spots in the sample. It is obvious that the spots are located in several chondrules.

The glow curves of six square portions I~VI in Figs. 1b and c were analyzed by two-dimensional photon counting method (YAMAMOTO et al., 1987). The glow curves are illustrated in Figs. 2a–f. We can find two types of glows in this sequence of TL image. The TL glow curves of the square portions II, V, and VI (hereafter, group A) have low temperature peaks (Figs. 2b, e, and f). On the other hand, those of portions I, III and IV (hereafter, group B) have high temperature peaks (Figs. 2a, c, and d). Positions of the peak temperature of the former and the latter are located around 80–120°C and 240–280°C, respectively. The glow curves of group A are essentially the same as those due to mesostases enriched in plagioclase component (NINAGAWA et al., 1991).
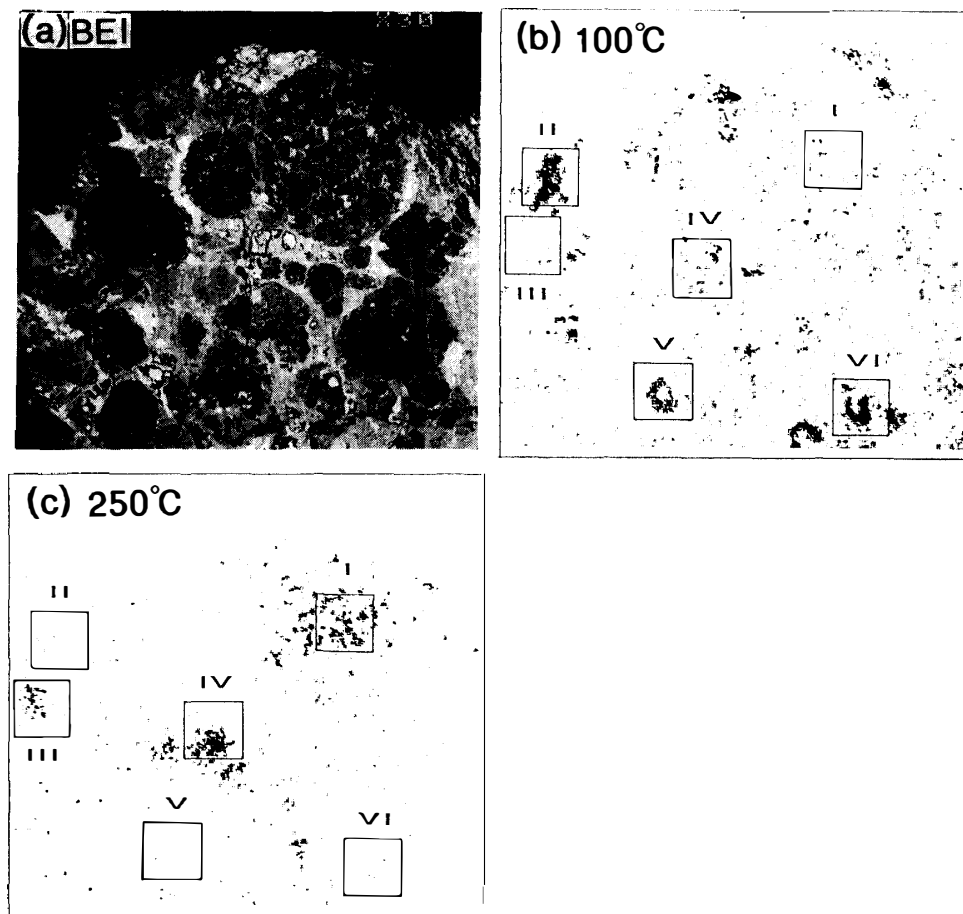

Fig. 1.   BEI and induced TL images of ALH-77214 (L3.4) chondrite. Long dimension is
2.9 mm. The position with high TL intensity is expressed by concentration of
black points. The slice sample was irradiated by γ-rays and received a dose of 13.2
kGy. (a) BEI of the slice sample of ALH-77214; (b) TL image at the temperature
interval 100–110°C; (c) TL image at the temperature interval 250–260°C. In Figs.
1b and c, the positions of square portions I, II, III, IV, V, and VI are also
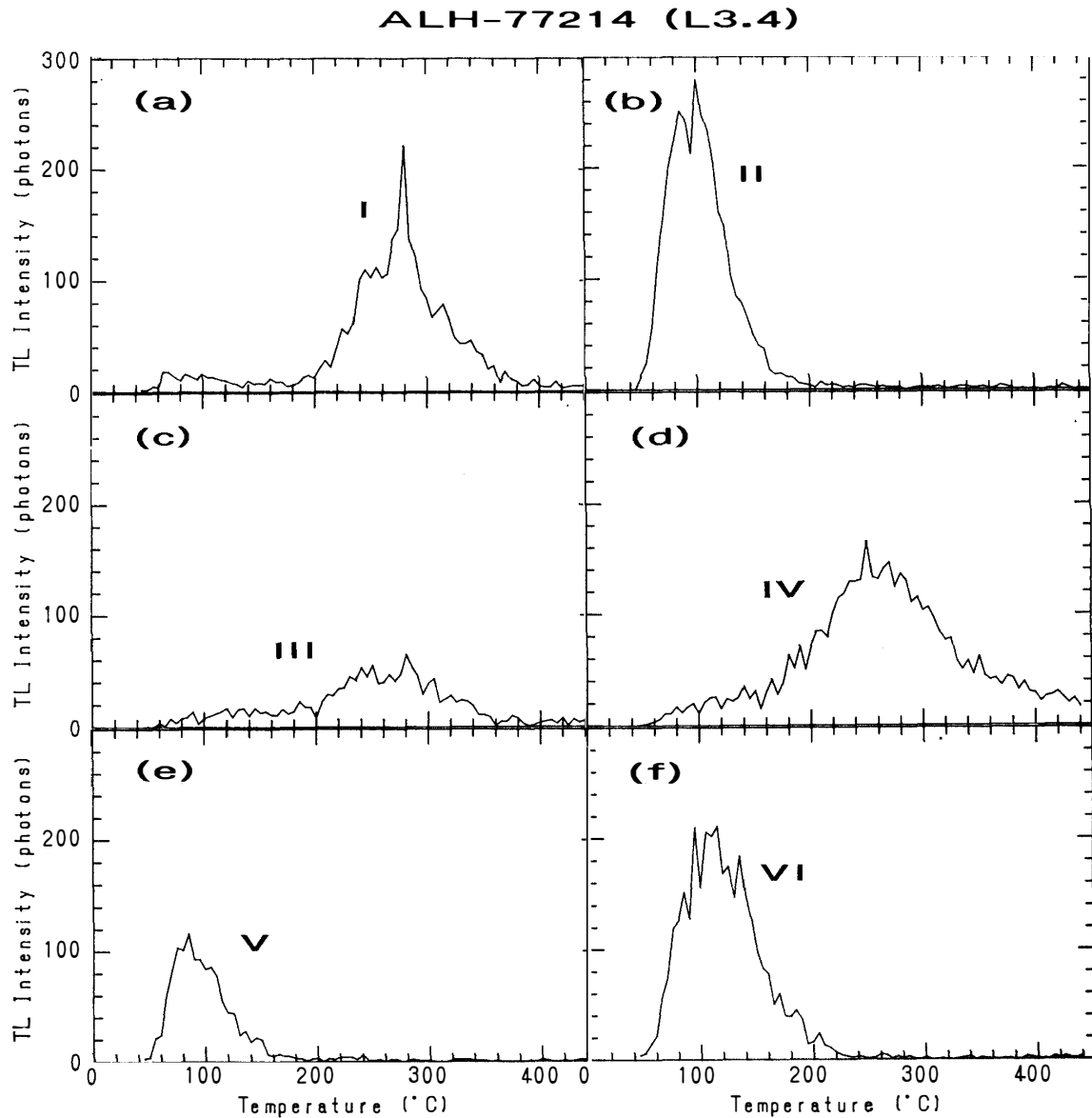displayed.

ALH-77214 (L3.4)

Fig. 2. TL glow curves of square portions I, II, III, IV, V, and VI in ALH-77214 (L3.4) chondrite, obtained by two-dimensional photon counting method. (a)I; (b)II; (c)III; (d)IV; (e)V; (f)VI.

3.2. Chemical compositions of the spots with intense TL

Enlarged views of portions I, II, III, and IV are shown in Figs. 3a–d. The mode of occurrence and chemical compositions of spots with intense TL emission are briefly described for Group A and Group B, respectively.

Group A: The TL emission regions in portion II are included in a porphyritic olivine-pyroxene chondrule (Fig. 3a). They mostly coincide with mesostasis of the chondrule. A large olivine phenocryst shows compositional zoning from core ($Fa_{6.9}$) to rim ($Fa_{21.6}$). Small low-Ca pyroxene crystals ($Wo_{0.8-2.7}Fs_{1.3-11.0}En_{86.3-97.9}$) are embedded in mesostasis. The mesostasis contains SiO_2 55.1–57.7 wt%, Al_2O_3 9.5–18.4 wt%, CaO 9.5–14.2 wt% and Na_2O 2.1–4.8 wt%. Relatively large variations
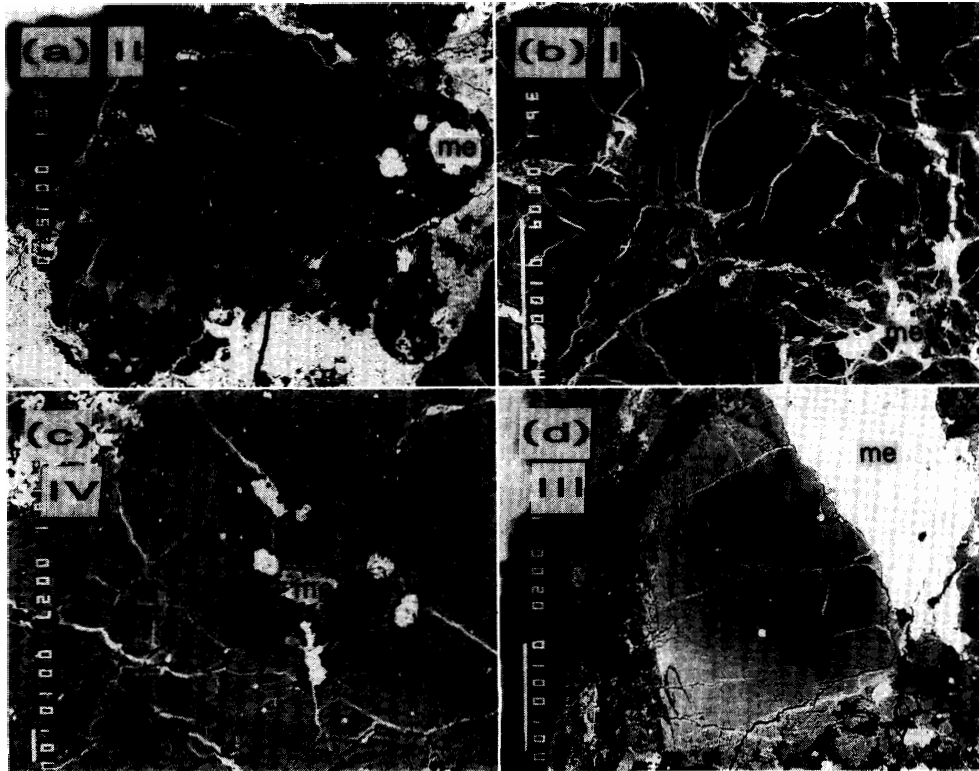
Fig. 3. Enlarged views of square portions I, II, III, and IV in ALH-77214 (L3.4) chondrite. (a) BEI of square portion II: a porphyritic olivine pyroxene chondrule. White bar 100 μm. (b) BEI of square portion I: a pyroxene chondrule with silica inclusions. White bar 100 μm. (c) BEI of square portion IV: a pyroxene chondrule with silica inclusions. White bar 10 μm. (d) BEI of square portion III: silica-rich mesostasis of a porphyritic olivine chondrule. White bar 100 μm. ol: olivine, px: low-Ca pyroxene, me: metallic Fe-Ni, si: silica phase, m: mesostasis.

of the Al_2O_3, CaO, and Na_2O contents are probably due to heterogeneous distribution of tiny grains of Ca-rich pyroxene dendrite in mesostasis. Average chemical composition of the mesostasis and the C.I.P.W. norm are listed in Table 1. The mesostasis in portion II is enriched in plagioclase component. The objects with high TL in portions V and VI are mesostases of porphyritic olivine-pyroxene chondrules. EPMA analyses show that they are also enriched in plagioclase component. The averages of chemical compositions of these mesostases in portions V and VI are also tabulated in Table 1. Compositional ranges of olivine and pyroxene are as follows: ol ($Fa_{5.2-20.8}$), low-Ca pyroxene ($Wo_{1.2-1.8}Fs_{1.5-3.2}En_{92.0-97.3}$) for chondrule in portion V; ol ($Fa_{17.7-25.2}$), low-Ca pyroxene ($Wo_{0.3-1.9}Fs_{6.0-18.0}En_{79.2-83.6}$) for chondrule in portion VI.

Group B: The objects with intense TL in portion I are distributed mostly in the central part of a pyroxene chondrule. They show round to prolate shapes with long dimensions ranging from 10 to 80 μm, and are embedded in boundaries between pyroxene crystals or included in pyroxenes (Fig. 3b). EPMA analysis revealed that these objects with the high temperature peak are silica phase ($SiO_2 =$ 97.3–99.5 wt%) with minor amounts of iron (0.5–1.9 wt% FeO) and MgO

(<0.4 wt%). Average composition of the silica phase is also tabulated in Table 1. Compositional range of pyroxene is $Wo_{1.2-1.5}Fs_{14.4-17.9}En_{80.7-84.3}$. The objects with intense TL in portion IV show similar mode of occurrence to those in portion I (Fig. 3c) and are also silica phase included in a pyroxene chondrule ($SiO_2 = 96.5$–97.6 wt%; $Al_2O_3 = 0.3$–1.5 wt%; $FeO = 0.9$–2.4 wt%; $MgO = 0.3$–0.4 wt%). Although the objects with intense TL in portion III have a similar glow curve to those of portions I and IV, the former shows a different mode of occurrence to the latter, and is silica-rich mesostasis of a porphyritic chondrule with large olivine phenocryst having a compositional zoning from core ($Fa_{21.4}$) to rim ($Fa_{34.7}$) (Fig. 3d). The compositional range of the mesostasis is $SiO_2 = 80.8$–86.0 wt%, $Al_2O_3 =$ 5.4–5.7 wt%, $FeO = 3.0$–4.1 wt%, $MgO = 2.9$–4.2 wt%, $CaO = 0.4$–0.9 wt% and $Na_2O = 1.6$–4.3 wt%. The average composition is also listed in Table 1.

Table 1. *Average chemical compositions and the C.I.P.W. norms of mesostases and silica-rich phases of six chondrules with intense TL in the ALH-77214 (L3.4) chondrite. Recalculated to total 100 wt%.*

Portion	II Mesostasis	V Mesostasis	VI Mesostasis	I Silica	IV Silica	III Silica-rich mesostasis
N*1	6	2	3	7	3	3
SiO_2	56.4	54.2	60.5	98.8	97.0	83.8
TiO_2	.40	.38	.47	—*2	—	.13
Al_2O_3	15.9	18.7	18.8	—	.71	5.58
Cr_2O_3	.42	.09	.13	—	—	.10
FeO*3	3.61	1.98	4.16	.91	1.54	3.46
MnO	.27	.13	.10	—	—	.10
MgO	8.04	8.42	1.69	.15	.35	3.71
CaO	10.8	12.4	4.26	—	.07	.56
Na_2O	3.93	3.35	9.32	—	.16	2.51
K_2O	.13	.17	.07	—	.06	.06
NiO	.13	.10	.44	.08	—	—
Q	1.16	—	—	97.59	93.89	59.37
C	—	—	—	—	.26	.37
or	.77	1.01	.41	—	.36	.36
ab	33.26	28.35	68.40	—	1.35	21.24
an	25.25	35.51	9.23	—	.35	2.78
ne	—	—	5.67	—	—	—
di-wo	11.83	10.88	4.97	—	—	—
en	8.24	8.38	1.79	—	—	—
fs	2.61	1.34	3.29	—	—	—
hy-en	11.79	9.76	—	.36	.87	9.24
fs	3.73	1.56	—	1.74	2.87	6.26
fo	—	1.98	1.69	—	—	—
fa	—	.35	3.42	—	—	—
cm	.62	.13	.19	—	—	.15
il	.76	.72	.89	—	—	.25
ab/(ab+an/2)*4	.58	.46	.89	—	.86	.89

*1: number of averaged analyses; *2: not detected; *3: total Fe as FeO; *4: molar ratio of normative minerals.

Table 2. List of silica samples for induced TL measurements.

| Sample	Description	Source
α-quartz (hydrothermal)	Single crystal	Otome Mine in central Honshu, Japan
α-quartz (volcanic)	Single crystal	Matsunosawa pyroclastic flow deposit of Haruna Volcano in the Northern Kanto, Japan
Tridymite	Polycrystal	Synthesized
Cristobalite	Polycrystal	Unknown locality in U.S.A.
Silica glass	Amorphous	Heraeus Co., Germany (Suprasil)
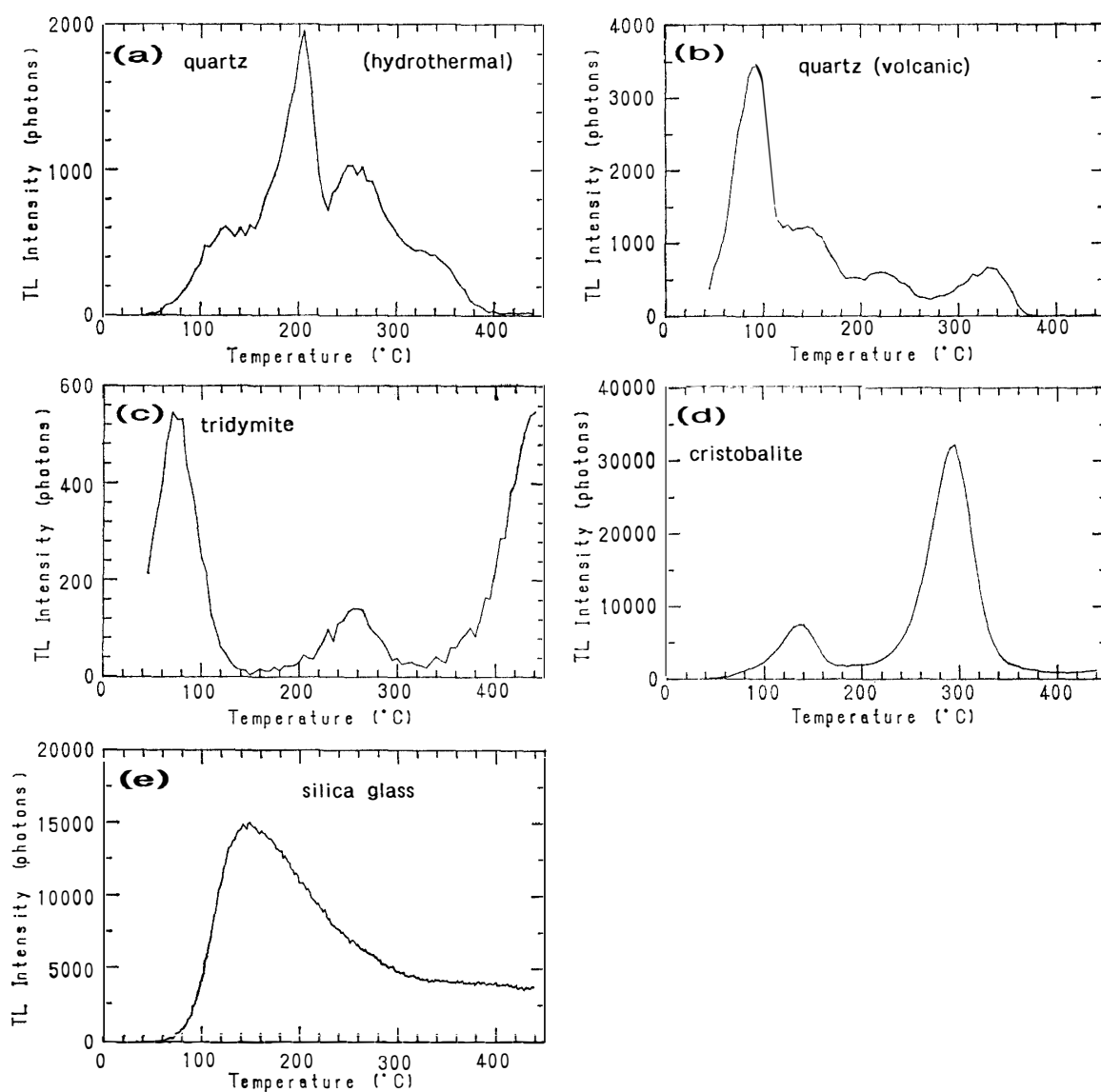
Fig. 4. TL glow curves of five silica phases. (a) hydrothermal quartz from the Otome Mine, irradiated by γ-rays and received a dose of 1.5 kGy; (b) volcanic quartz from the Haruna Volcano, irradiated by γ-rays and received a dose of 1.5 kGy; (c) synthesized tridymite, irradiated by γ-rays and received a dose of 10.8 kGy; (d) cristobalite from the U.S.A., irradiated by γ-rays and received a dose of 1.5 kGy; (e) silica glass, irradiated by γ-rays and received a dose of 1.5 kGy.

The other luminous parts in Figs. 1b and c are interpreted to be corresponding to the TL emission due to silica phase and chondrule mesostases enriched in plagioclase or silica component.

3.3. Tentative identification of the silica polymorph

In order to identify a polymorph of the silica phase in portions I and IV, we measured glow curves of induced TL of five silica samples (hydrothermal quartz, volcanic quartz, synthesized tridymite, cristobalite, and silica glass) (Table 2). The silica glass was checked to be amorphous using usual X-ray diffraction method. They were also irradiated by ^{60}Co γ-rays. Quartz, cristobalite, and silica glass received a dose of 1.5 kGy. Tridymite received a dose of 10.8 kGy. The glow curves of their induced TL are shown in Figs. 4a–e. The glow curves of both α-quartz crystals (hydrothermal and volcanic) are characterized by four peaks. The glow curve of synthesized tridymite is characterized by three peaks. The glow curve of cristobalite is characterized by two peaks: a small peak at low temperature ($\sim$140°C) and a large peak at high temperature ($\sim$290°C). The glow curve of silica glass is characterized by both single low temperature peak and broad continuum of emission at higher temperatures. Comparing these glow curves with that of silica phase in portion I, it is noticed that it also has two peaks: a small peak at low temperature (around 100°C) and a large peak at high temperature (around 280°C). The glow curves of the silica phase and cristobalite are similar in shape, although peak temperatures of them are slightly different from each other. This suggests that the silica phase may be cristobalite.

4. Discussion

4.1. Effects of dose and heating rate on glow curve shape

In this paper, we reported only the results of irradiation of a large dose of 13.2 kGy and heating rate 0.25°C/s. The measurements of TL sensitivity (SEARS et al., 1980, 1982, 1991) have been performed with irradiation of a dose of about 0.25 kGy and at heating rate about 7.5°C/s (SEARS et al., 1982; KECK and SEARS, 1987). Here, we briefly mention effects of dose and heating rate on glow curve shape. Powder sample of the ALH-77214 (L3.4) chondrite (20 mg) was irradiated by ^{60}Co γ-rays. Effect of dose were investigated in the two cases of 13.2 kGy and 0.2 kGy. The TL measurements were conducted immediately after γ-rays irradiation at two different rates of heating, 0.25°C/s and 7.5°C/s, with Corning band pass filters 7–59 and 4–69 in nitrogen atmosphere. The glow curves were measured by a usual photon counting method with a photomultiplier.

Figures 5a and b illustrate the effect of dose for measurements at the heating rate of 0.25°C/s. Figure 5a clearly shows a large peak at 110°C and a small peak at 260°C. It is considered that they correspond to that due to mesostases enriched in plagioclase component and that due to silica phases, respectively. In the case of a dose of 0.2 kGy, we can observe only the TL signal with a peak at about 110°C, which is also corresponding to that from chondrule mesostases enriched in plagio-clase component (Fig. 5b). In Section 3 we described the TL signals of the silica
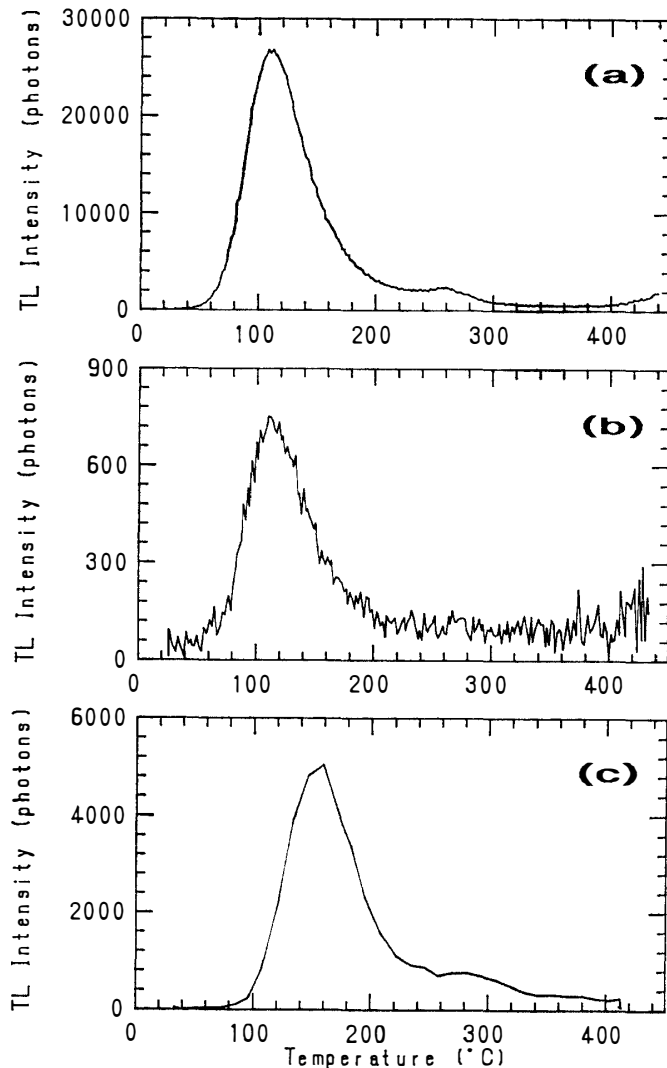
Fig. 5 Effects of dose and heating rate on glow curve shape. Powder sample of ALH-77214 (L3.4) chondrite (20 mg) was irradiated by ^{60}Co γ-rays. Effects of dose were investigated in the two cases of 13.2 kGy and 0.2 kGy. The TL measurements were conducted immediately after γ-rays irradiation at two different heating rates, 0.25°C/s and 7.5°C/s, with Corning band pass filters 7–59 and 4–69 in nitrogen atmosphere. The glow curves were measured by a usual photon counting method with a photomultiplier. (a) 13.2 kGy, 0.25°C/s; (b) 0.2 kGy, 0.25°C/s; (c) 0.2 kGy, 7.5°C/s.

phase with peaks at 240–280°C in the case 13.2 kGy and 0.25°C/s (Figs. 2a, c, and d). However, we can hardly detect them in the case 0.2 kGy and 0.25°C/s (Fig. 5b).

Figures 5b and c display the effect of heating rate in the case of a dose of 0.2 kGy. The glow curve shape in the case of 0.2 kGy and 7.5°C/s (Fig. 5c) is similar to that in the case of 13.2 kGy and 0.25°C/s (Fig. 5a). It is worth noting that the former also has a large peak at 160°C and a small peak at 280°C.

From these data, TL signals in the case of 13.2 kGy for chondrule mesostases enriched in plagioclase component and silica phases are essentially not different from those in the case of 0.2 kGy. It is concluded that in the case of irradiation by a dose of 13.2 kGy and heating rate of 0.25°C/s we can obtain the same TL characteristics as those observed in usual measurements of TL sensitivity (Sears *et al.*, 1980, 1982, 1991).

4.2. Silica phases as a common TL phosphor in chondritic meteorites

As already described by many authors, minor silica phases are commonly

observed in chondrules and clasts from carbonaceous, ordinary, and enstatite chondrites. OLSEN (1983) reported two enstatite-silica chondrules from the Murchison carbonaceous chondrite. They contain segregations of glass that are essentially pure silica. PLANNER (1983) described a silica-bearing low-Ca pyroxene chondrule fragment from Piancaldoli (LL3). The fragment contains prolate silica spheroids embedded in a matrix with an approximate low-Ca pyroxene (Fs_{14}) composition. He showed that many of the silica spheroids contain dendritic cristobalite. BRIGHAM et al. (1986) have published detailed studies on silica-bearing low-Ca pyroxene chondrules and olivine clasts from several unequilibrated ordinary chondrites (UOCs). They have discussed the mechanisms of the silica-normative compositions for these components. CHRISTOPHE MICHEL-LÉVY (1988) reported silica-pyroxene microchondrules in Mezö-Madaras (L3) chondrite. In enstatite chondrites, minor silica phases are commonly found (KEIL, 1968). RUBIN (1983) reported silica-rich clasts in Adhi Kot enstatite chondrite breccia.

In the present study, the silica phases with intense TL are reported in three chondrules of ALH-77214 (L3.4) chondrite. There appear to be two distinct types: silica and low-Ca pyroxene assemblages, and olivine and silica-rich mesostasis assemblage. The silica and low Ca-pyroxene assemblages in portions I and IV are typical ones in silica-bearing chondrules of UOCs (BRIGHAM et al., 1986). PLANNER (1983) showed that many of the silica spheroids embedded in a matrix with pyroxene composition contain dendritic cristobalite, suggesting metastable coexistence of two liquid phases. Although the silica phases in portion I are tentatively identified as cristobalite, they seem to show no textural evidence for crystallization from liquid phases with silica composition. Cristobalite inclusions in portions I and IV may be a primary phase crystallized from melt droplets with silica-normative compositions.

The high silica-enrichment of the olivine chondrule mesostasis in portion III is considered to be a result of metastable crystallization of olivine due to rapid cooling of the chondrule melt. Rapid cooling causes delay of nucleation of pyroxene and enrichment of silica component in residual melt. The cristobalite in portion III may have crystallized from the mesostasis with highly silica-rich composition.

In ALH-77214 (L3.4) chondrite with low TL sensitivity, silica phases with intense TL are commonly detected as a minor TL phosphor in pyroxene chondrules and olivine chondrules with silica-normative compositions. It is also revealed that the silica phases have the characteristic TL signals. Since silica phases are commonly observed as a minor phase in enstatite, ordinary, and carbonaceous chondrites, they have an importance to TL studies of chondritic meteorites. Utilizing silica phases as a common TL phosphor, we can make a comparative study of TL characteristics (glow curve shape, intensity, and emission spectra) among chondritic meteorites to clarify differences of physical conditions in their formation environments such as chondrule formation and metamorphism.

Acknowledgments

References

Brigham, C. A., Yabuki, H., Ouyang, Z., Murrell, M. T., El Goresy, A. and Burnett, D. S. (1986): Silica-bearing chondrules and clasts in ordinary chondrites. Geochim. Cosmochim. Acta, **50**, 1655–1666.

Christophe Michel-Lévy, M. (1988): A new component of the Mezö-Madaras breccia: A microchondrule- and carbon-bearing L-related chondrite. Meteoritics, **23**, 45–48.

Keck, B. D. and Sears, D. W. (1987): Chemical and physical studies of type 3 chondrites—VIII: Thermoluminescence and metamorphism in the CO chondrites. Geochim. Cosmochim. Acta, **51**, 3013–3021.

Keil, K. (1968): Mineralogical and chemical relationships among enstatite chondrites. J. Geophys. Res., **73**, 6945–6976.

Ninagawa, K., Yamamoto, I., Wada, T., Matsunami, S. and Nishimura, H. (1990): Thermo- luminescence study of ordinary chondrites by TL spatial distribution readout system. Proc. NIPR Symp. Antarct. Meteorites, **3**, 244–253.

Ninagawa, K., Kubo, H., Fujimura, S., Yamamoto, I., Wada, T., Matsunami, S. and Nishi- mura, H. (1991): Thermoluminescence characteristics and chemical compositions of mesostases in ordinary chondrites. Proc. NIPR Symp. Antarct. Meteorites, **4**, 344–351.

Olsen, E. J. (1983): SiO_2-bearing chondrules in the Murchison (C2) meteorite. Chondrules and Their Origins, ed. by E. A. King. Houston, Lunar Planet. Inst., 223–234.

Planner, H. N. (1983): Phase separation in a chondrule fragment from the Piancaldoli (LL3) chondrite. Chondrules and Their Origins, ed. by E. A. King. Houston, Lunar Planet. Inst., 235–242.

Rubin, A. E. (1983): The Adhi Kot breccia and implications for the origin of chondrules and silica-rich clasts in enstatite chondrites. Earth Planet. Sci. Lett., **64**, 201–212.

Sears, D. W. (1988): Thermoluminescence of meteorites: Shedding light on the cosmos. Nucl. Tracks Radiat. Meas., **14**, 5–17.

Sears, D. W. and Weeks, K. S. (1983): Chemical and physical studies of type 3 chondrites—II; Thermoluminescence of sixteen type 3 ordinary chondrites and relationships with oxygen isotopes. Proc. Lunar Planet. Sci. Conf., 14th, Pt. 1, B301–B311 (J. Geophys. Res., **88** Suppl.).

Sears, D. W., Grossman, J. N., Melcher, C. L., Ross, L. M. and Mills, A. A. (1980): Measur- ing metamorphic history of unequilibrated ordinary chondrites. Nature, **287**, 791–795.

Sears, D. W., Grossman, J. N. and Melcher, C. L. (1982): Chemical and physical studies of type 3 chondrites—I; Metamorphism related studies of Antarctic and other type 3 ordinary chondrites. Geochim. Cosmochim. Acta, **46**, 2471–2481.

Sears, D. W., Sparks, M. H. and Rubin, A. E. (1984): Chemical and physical studies of type 3 chondrites—III; Chondrules from the Dhajara H3.8 chondrite. Geochim. Cosmochim. Acta, **48**, 1189–1200.

Sears, D. W., Hasan, F. A., Batchelor, J. D. and Lu, J. (1991): Chemical and physical studies of type 3 chondrites—XI; Metamorphism, pairing, brecciation of type 3 ordinary chondrites. Proc. Lunar Planet. Sci., **21**, 493–512.

Yamamoto, I., Imaeda, K., Takahashi, N., Ninagawa, K., Tomiyama, T., Wada, T. and Yama- shita, Y. (1987): Spatial distribution readout system of thermoluminescence sheet II. Nucl. Instrum. Methods, **A256**, 567–575.